

# Hysteresis as a Probe of Turbulent Bifurcation in Intrinsic Rotation Reversals on Alcator C-Mod

N. M. Cao<sup>1</sup>, J.E. Rice<sup>1</sup>, P.H. Diamond<sup>2</sup>, A.E. White<sup>1</sup>, S.G. Baek<sup>1</sup>, M.A. Chilenski<sup>1</sup>, J.W. Hughes<sup>1</sup>, J. Irby<sup>1</sup>, M.L. Reinke<sup>3</sup>, P. Rodriguez-Fernandez<sup>1</sup> and the Alcator C-Mod Team

<sup>1</sup> Massachusetts Institute of Technology (MIT), Cambridge, MA, USA

<sup>2</sup> University of California, San Diego (UCSD), San Diego, CA, USA

<sup>3</sup> Oak Ridge National Laboratory (ORNL), Oak Ridge, TN, USA

**Abstract.** Analysis and modeling of a new set of rotation reversal hysteresis experiments unambiguously show that changes in turbulence are responsible for the intrinsic rotation reversal and the Linear to Saturated Ohmic Confinement (LOC/SOC) transition on Alcator C-Mod. Plasmas on either side of the reversal exhibit different toroidal rotation profiles and therefore different turbulence characteristics despite profiles of density and temperature that are indistinguishable within measurement uncertainty. The deactivation of subdominant (in linear growth rate and heat transport) ITG and TEM-like instabilities in a mixed-mode state is identified as the only possible change in turbulence within a quasilinear transport approximation across the reversal which is consistent with the measured profiles and the inferred heat and particle fluxes. This indicates an explanation for the LOC/SOC transition that provides a mechanism for hysteresis through the dynamics of subdominant modes and changes in their relative populations, and does not involve a change in most (linearly) unstable ion-scale drift-wave instability.

The universally observed connection of the Linear to Saturated Ohmic Confinement (LOC/SOC) transition with the intrinsic rotation reversal in Ohmic L-mode plasmas is a longstanding mystery in fusion plasmas [1, 2, 3, 4]. The concurrence of these two transitions suggests a link between the heat, particle, and momentum transport channels in tokamak plasmas, reminiscent of how heat-flux driven turbulent Reynolds stresses are thought to trigger the L-H transition, and lead to shear layer and pedestal formation [5]. While there has been success in modeling the energy and particle transport of the LOC/SOC transition [6, 7, 4], a self-contained picture of how the changes in turbulence lead to the rotation reversal and explain its observed properties remains elusive. Here, we propose a partial turbulence population collapse, which involves the deactivation of a subdominant instability, as a possible mechanism underlying the Ohmic rotation reversal.

The LOC/SOC transition refers to a break in the slope of energy confinement time when plotted against density and is observed in tokamak L-mode plasmas. This confinement transition is accompanied by a reversal in intrinsic core toroidal rotation. This reversal is a spontaneous reorganization of the plasma rotation from co-current to counter-current with no external momentum input. Additionally, many experiments reveal changes in fluctuations across the LOC/SOC transition [2, 8, 9]. Taken together, these observations suggest that rotation reversal and energy confinement saturation are linked through the dynamics of drift wave turbulence.

It is thought that a transition from trapped electron mode (TEM) to ion-temperature gradient (ITG) mode dominated turbulence could unify the confinement transition and rotation reversal [6, 10, 11]. It has been established that the observed rotation profiles require some form of turbulent symmetry breaking [12, 13, 14, 15, 11] which allows for the conversion of free energy released by heat transport to up-gradient momentum transport [16, 17]. Nonlinear global gyrokinetic simulation has confirmed that the direction of rotation can flip between TEM and ITG dominated regimes, and can match the magnitude of rotation observed [18, 19, 20, 4]. However, analysis of C-Mod and AUG plasmas do not always show a change in dominant linear instability between ITG/TEM at the LOC/SOC transition or rotation reversal [21, 22, 7, 23]. Additional insight is needed to elucidate how the ITG/TEM transition is involved in the rotation reversal, as a transition in growth rate or heat flux dominance does not explain the momentum transport bifurcation.

In this work, a set of experiments is presented that uses hysteresis as a novel probe of the LOC/SOC transition and intrinsic rotation reversal. Hysteresis is the dependence of a system's state on its history, and could be the result of memory or the evolution of hidden variables not tracked in the state space. Hysteresis in rotation of L-mode plasmas has been observed on several different experiments [24, 25]. The experiment presented here shows that nearly exact matches of mean density and temperature profiles can lead to different rotation and turbulent states in the same discharge. This shows that directly measured profile effects or other parametric dependencies of the turbulent response are not responsible for the transition itself, and instead must be the result of a nonlinear

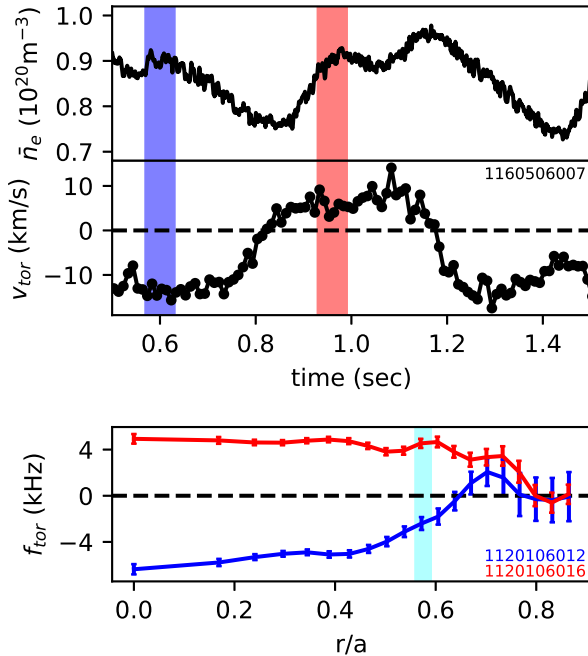


**Figure 1.** Time trace of a representative discharge from the hysteresis experiments (top) and representative toroidal rotation profiles (bottom). The two times marked by the blue and red bars have nearly the same line-average density, electron and ion temperatures, but different core toroidal velocities. Toroidal rotation profiles are shown from a different but matched set of shots. The rotation is similar at the edge but diverges in the core. Simulations were run within the highlighted region.

bifurcation in the turbulent state.

The experiments were run on Alcator C-Mod, a compact ( $R = 0.67\text{m}$ ,  $a = 21\text{cm}$ ), high-field ( $B_t$  up to 8.1 T) diverted tokamak with a molybdenum wall [26]. To realize the hysteresis, active line-average density control with edge fueling and a cryopump, along with the C-Mod two-color interferometer system, were used to create density modulations. These modulations were triangle waves with amplitude  $\pm 10\%$  of a central value, and period much longer than the energy confinement time,  $600\text{ms} \gg \tau_e \approx 25\text{ms}$ . Rotation profiles also evolved on timescales  $\sim \tau_e$ , slower than the modulation period. These plasmas were Ohmic upper single null,  $B_t = 5.4$  T,  $I_p = 0.8$  MA discharges. There was no beam injection in these plasmas, so the only particle source is at the edge. Additionally, on some discharges CaF2 impurity was injected into the plasma using a laser blow-off (LBO) system. Time traces from a representative discharge are shown in Figure 1. The plasma core is observed to rotate co-current in the lower collisionality LOC branch, and counter-current in the higher collisionality SOC branch.

Hysteresis can be visualized by plotting discharge trajectories in the density-rotation plane, as is done in Figure 2. The plotted trajectories overlay closely, showing the robustness of the hysteresis phenomenon to noise and perturbation from LBO. Kinetic profiles matched across the reversal are shown in Figure 3. Electron density and

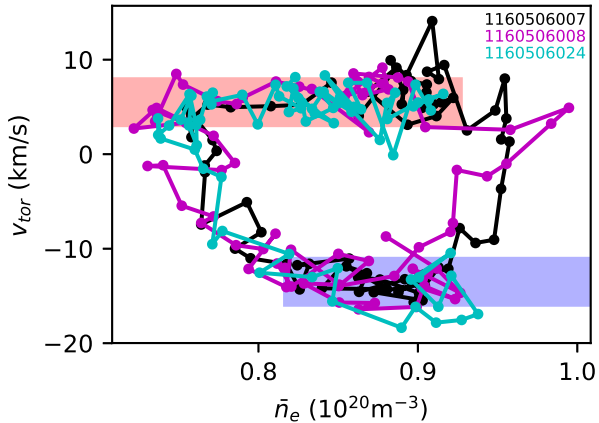


**Figure 2.** Trajectories of several discharges at two different currents plotted in the density vs. toroidal velocity plane. Each point is a timeslice, 10 ms apart. The regions in phase space corresponding to LOC and SOC branches are highlighted in red and blue respectively. The discharge in cyan does not reach a high enough density to transition from co-current rotation to counter-current rotation, so it does not form a closed hysteresis loop.

temperature were measured using both the core and edge Thomson scattering systems at C-Mod, while core  $T_e$  was also measured with the GPC ECE system. The data were time-averaged over 60 ms bins, then fused into smooth analytic profiles using Gaussian Process Regression to provide rigorous estimates of the profiles, gradients, and their errors [27]. Note these error estimates include both statistical and systematic uncertainties. The tanh length scale shape and hyperprior form in Table 1 of [27] were used in the fit, and Markov Chain Monte Carlo used to marginalize out the hyperparameters. Only line-integrated ion temperature and rotation were available for this set of discharges, so ion temperature and rotation profiles were used from previously published LOC/SOC transition experiments on C-Mod whose experimental parameters were replicated in this set of experiments [28]. The profiles, and in particular the gradients which serve as linear drives for the drift-wave turbulence, overlay each other very closely, which indicates that drift-wave linear stability does not change across the reversal.

Linear CGYRO [29] was used to find the most unstable eigenmodes over a range of  $k_y \rho_s$  for the matched LOC/SOC conditions, as well as in the conditions leading up to the transition. Both ions and electrons were fully gyrokinetic, and  $\delta A_{\parallel}$  fluctuations were included.  $Z_{eff}$  was calculated from neoclassical resistivity. These simulations were run at multiple radii, and over both ion and electron scales. The real frequency and growth rates calculated in these simulations are shown in Figure 3.

At nominal values of the gradients, the linear stability analysis does not show evidence of a transition from ion-direction to electron-direction dominance, either for the matched LOC/SOC profiles, or right before the transitions. This is consistent with

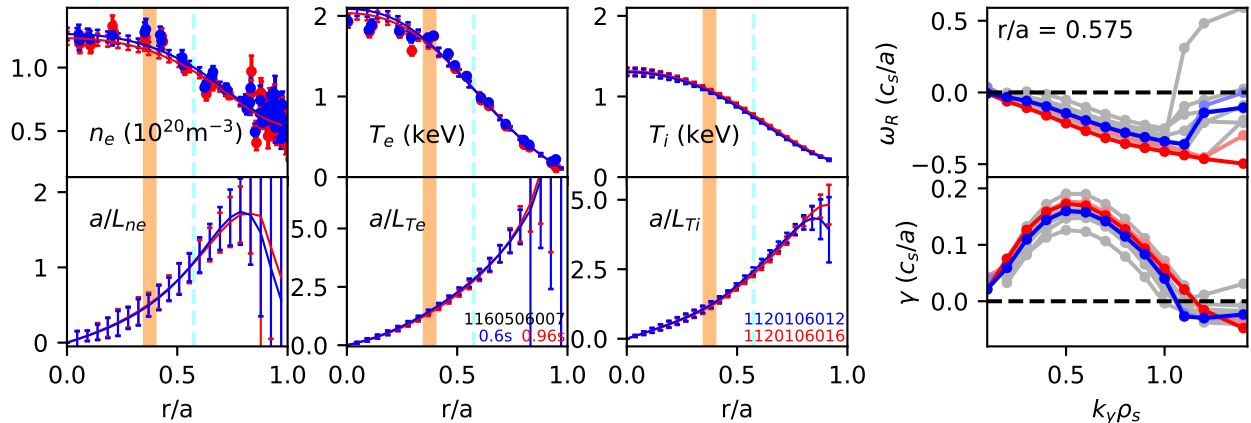


**Figure 3.** (LEFT) Profiles of electron density, electron temperature, and ion temperature and respective gradient scale lengths for the 0.8 MA case, for co-current LOC branch (red) and counter-current SOC branch (blue). The raw data is shown by the scatter points, and the fitted profiles with a smooth line. The orange shaded region is the approximate sawtooth inversion radius, and the dashed cyan line shows the location of the CGYRO simulations. (RIGHT) Real frequency (top) and growth rate (bottom) of most unstable mode at different  $k_y \rho_s$ . Several cases are plotted; the dark blue and dark red correspond to the matched profile conditions for counter-current and co-current cases respectively. The light blue and light red correspond to conditions right before transition, and also do not show qualitative difference in stability. The gray corresponds to variation of the driving gradients within error bars from the counter-current matched case.

linear stability analyses of databases Ohmic C-Mod and AUG discharges, which have not shown a clear correlation between TEM $\leftrightarrow$ ITG dominance transition and either the LOC/SOC transition or the rotation reversal [21, 22, 23, 30, 7]. This radial location  $r/a = 0.575$  remains ITG dominant when varying a single driving gradient within error bars, although variation outside of one standard deviation from the nominal value can lead to TEMs overtaking ITGs in growth rate, indicating that the plasma remains near a TEM $\leftrightarrow$ ITG dominance transition. These results suggest that the behavior of modes beyond the dominant linear instability is involved in the transition, which motivates us to look at the contribution of subdominant modes. In the following, subdominant modes refer to modes which are the fastest growing mode at some  $k_y \rho_s$ , but which have lower growth rates or effect subdominant levels of heat transport than the dominant ITG instability.

To diagnose the turbulent state of the plasma, a reduced model is constructed using a linear mode quasilinear transport approximation (mQLTA). In mQLTA, the turbulent fluxes (e.g.  $Q_e$ ) are calculated by the sum of a quasilinear mode weight (denoted below as  $W_{Q_e,k}$ ) times an average intensity (also called spectral weight, denoted  $\langle \bar{\phi}_k^2 \rangle$ ) for each

linear eigenmode indexed by wavenumber  $k$ ,

$$Q_e = \sum_k W_{Qe,k} \langle \bar{\phi}_k^2 \rangle \quad (1)$$

This model separates the linear physics of the plasma, encoded into quasilinear weights assumed to be determined entirely by the linear mode structures, from the nonlinear physics, encoded into the spectral weights which are determined by nonlinear saturation processes. While the theoretical validity of this assumption has not been established, in practice the weights used in mQLTA have been found to match weights from fully nonlinear simulation [31]. Additionally, the predicted cross-phases, which are related to the quasilinear weights, have been observed to match experimental measurements [32, 33]. This model also underlies modern quasilinear transport models like TGLF [34] and QualiKiz [35], which have had success in replicating heat and particle transport in LOC/SOC transition scans [7, 4].

By using the fluxes calculated from power balance, it is possible to put an experimentally-derived constraint on the possible mode intensities. Three fluxes are used: the ion and electron heat fluxes, and the electron particle flux. Equation 1 can then be viewed as a matrix equation relating a vector of mode intensities to a 3-dimensional vector of fluxes. If the system is discretized into  $N$  modes, then the quasilinear weights form a  $3 \times N$  matrix, as in the first line of equation 2.

$$\begin{bmatrix} Q_i \\ Q_e \\ \Gamma_e \end{bmatrix} = \begin{bmatrix} W_{Qi,k_1} & W_{Qi,k_2} & \dots \\ W_{Qe,k_1} & W_{Qe,k_2} & \dots \\ W_{\Gamma e,k_1} & W_{\Gamma e,k_2} & \dots \end{bmatrix} \begin{bmatrix} \langle \bar{\phi}_{k_1}^2 \rangle \\ \langle \bar{\phi}_{k_2}^2 \rangle \\ \vdots \end{bmatrix} \approx \begin{bmatrix} W_{Qi,Ia} & W_{Qi,Ib} & W_{Qi,II} & W_{Qi,III} \\ W_{Qe,Ia} & W_{Qe,Ib} & W_{Qe,II} & W_{Qe,III} \\ W_{\Gamma e,Ia} & W_{\Gamma e,Ib} & W_{\Gamma e,II} & W_{\Gamma e,III} \end{bmatrix} \begin{bmatrix} \langle \bar{\phi}_k^2 \rangle_{Ia} \\ \langle \bar{\phi}_k^2 \rangle_{Ib} \\ \langle \bar{\phi}_k^2 \rangle_{II} \\ \langle \bar{\phi}_k^2 \rangle_{III} \end{bmatrix} \quad (2)$$

In the full system,  $N$  will be very large, so a naive application of the constraint leaves the mode intensities highly underdetermined. However, we are not interested in the detailed shape of the spectrum, only trends in intensities and fluxes. This motivates the construction of a reduced model where similar modes are lumped into ‘families’. For example, ETG modes primarily exhaust electron heat flux, and do not exhaust ion heat flux or particle fluxes. Thus, only one degree of freedom is required to describe the net effect of ETG modes on the fluxes. To calculate the fluxes due to families, the sum over modes  $k$  in equation 1 is replaced instead with a sum over families, with a representative quasilinear weight averaged over the modes comprising the family, as in the second line of equation 2.

To apply this model to the experiment, quasilinear weights were calculated from the linear CGYRO runs on the matched conditions. The gyro-Bohm normalized weights are plotted in Figure 4 for the counter-current rotation simulations, with the co-current

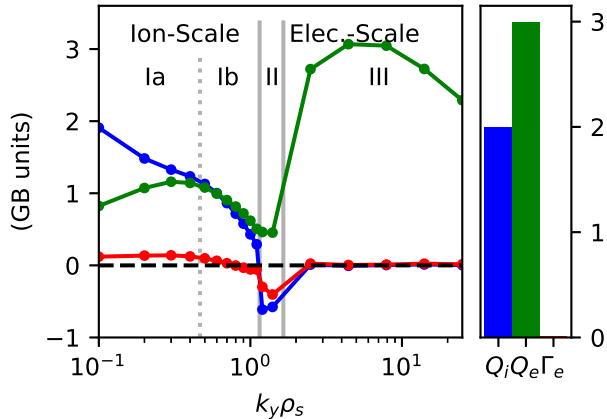


**Figure 4.** The quasilinear weights are shown for the most unstable drift wave modes from the 0.8 MA matched profile counter-current SOC branch case over a range of  $k_y \rho_s$  (left). The anomalous fluxes at the corresponding radial location are shown in the bar chart (right). The units are gyro-Bohm normalized, and the quasilinear weights correspond to the fluxes of the same color. The four mode families are labeled Ia, Ib, II, and III.

**Table 1.** Summary of the consequences of the two possible turbulent states predicted by mQLTA.

Turbulent State	LOC	SOC
Active Mode Families	ITG (Ia, Ib) TEM (II) ETG (III)	ITG (Ib) ETG (III)
Particle Flux Balance	Ia balances II	Balance within Ib
Electron Heat Transport	TEM and ETG	ETG dominates
Torque Balance	TEM and ITG	ITG dominates

rotation simulations having nearly identical weights. From here, four families of modes are identified. Family I consists of low- $k$  ion-direction modes, separated into (a) and (b) based on the efficiency of particle flux exhaust. The lower- $k$  modes are more effective at driving electron density flux down-gradient, while the higher- $k$  modes drive close to zero net electron density flux. Family II consists of marginally stable  $k_y \rho_s \sim 1$  hybrid direction TEM-like modes, and are characterized by their inward particle pinch. Family III consists of high- $k$  electron-direction modes, which exhaust only electron heat flux. The fluxes calculated from TRANSP power balance [36] are shown on the right in Figure 4, with neoclassical transport calculated by the code NEO [37] subtracted out.

The additional constraint that mode intensities must be non-negative distinguishes two qualitatively different types of solution of equation 2. The first is where  $\langle \bar{\phi}_k^2 \rangle_{II} \approx 0$ , so the marginally stable family II is not active. In order to satisfy the near-zero electron particle flux, the only ion-scale turbulence that can be active are modes in family Ib.

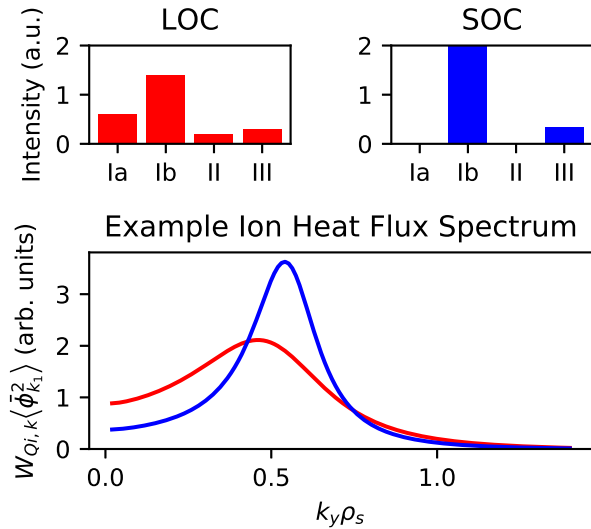


**Figure 5.** A qualitative illustration of the proposed LOC/SOC transition. (Top) the four mode family intensities are shown. In SOC family II is inactive, which necessarily shifts the balance of modes Ia and Ib. (Bottom) An example of an ion heat flux spectrum which would be consistent with the above mode families, where the SOC spectrum in blue is narrower than the LOC spectrum in red.

Modes in family III then exhaust the remaining electron heat flux. This leads to a narrower  $k$  spectrum of ion-scale turbulence, dominated by ion-direction turbulence, corresponding to a “SOC-like” case. The second possibility is where the modes in family II are active. Then, the lower- $k$  family Ia must be active as well, in order to balance the inward electron particle flux. This leads to a broader  $k$  spectrum with intermixed ion-direction and hybrid-direction turbulence, corresponding to a “LOC-like” case. Since the “LOC-like” and “SOC-like” states continuously connect to co-current rotation lower-collisionality and counter-current rotation higher-collisionality branches respectively, it is inferred that the rotation physics of TEM dominant (but possibly ITG active) and ITG dominant states continue to be relevant in their respective regimes. These changes are illustrated in Figure 5, and their consequences are summarized in Table 1. The implication is that despite the heat transport channels being the principal externally driven means of free energy release in the plasma, modes which are subdominant in heat transport can be central to determining the qualitative behavior of transport in other channels, such as that of momentum transport.

While this work does not provide a mechanism for the observed bistability of the turbulent state leading to the hysteresis, it does show that the bistability cannot be explained by changes in the linear turbulence drive terms alone. The robustness of the bistability to perturbation from LBO provides evidence against the possibility of the matched profiles sitting on an undetected linear stability boundary, given the large effect of LBO on turbulence in the plasma [38]. One possible mean field mechanism for bistability is the mean rotation profile feedback on turbulence saturation and coupling.

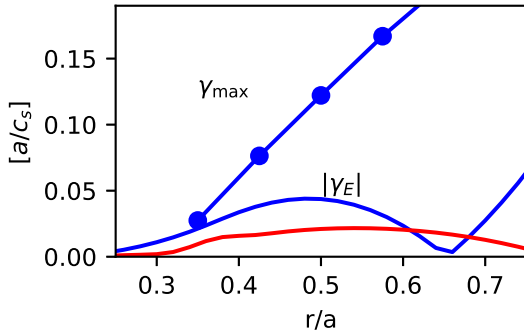


**Figure 6.** Plot of maximum growth rate for modes with  $k_y \rho_s < 1$  (solid line with dots) and  $\mathbf{E} \times \mathbf{B}$  shearing rate  $\gamma_E = \frac{r}{q} \frac{d\omega_0}{dr}$  (solid lines without dots) as a function of  $r/a$ , where  $\omega_0$  is calculated from force balance. For the shear, blue corresponds to SOC conditions and red to LOC conditions. Note that the maximum growth rate is above the  $\mathbf{E} \times \mathbf{B}$  shearing rate, but the shearing rate can be comparable to subdominant mode growth rates.

The ExB flow shear is not large enough to change the linear structure of the dominant instability, as seen from the CGYRO simulations, but is a significant fraction of the maximum growth rate as seen in Figure 6. Thus, it could affect the saturation of more marginally stable turbulence, or change turbulence spreading behavior. Another possibility is a mechanism outside of mean field theory, where some meso- or micro-scale field changes the mode-mode or mode-zonal flow nonlinear energy transfer. One such example is staircase formation [39]. Both of these possibilities resemble a ‘population collapse’ described by predator-prey models of turbulence, see e.g. [5]. However, in contrast to the L-H transition, where virtually all ion scale turbulence is quenched, here only a portion of the ion scale spectrum collapses at the transition. These changes could manifest in several ways experimentally, either directly in measured fluctuation spectra in the case of a total subdominant population quench, or indirectly through changes in measured fluctuation correlation lengths if some meso-scale phenomenon was responsible.

In summary, this work presents results from new hysteresis experiments which demonstrate density and temperature profiles, which are indistinguishable within error bars, leading to different turbulent and rotation states. Since the edge rotation is similar, core rotation profiles are self-consistently determined by the turbulence in the plasma, indicating that turbulence changes across the LOC/SOC transition. The observed kinetic profiles and robustness of hysteresis to perturbation places tight constraints on possible mechanisms for the rotation reversal, in particular showing that a change in linear turbulence drive terms alone cannot explain the rotation reversal or LOC/SOC transition on Alcator C-Mod. Linear gyrokinetic simulations at nominal values of the gradients show ITG to be linearly dominant throughout the hysteresis loop in the rotation reversal region, although the plasma remains close ( $\gtrsim 1$  standard deviation in gradient drives) to a linear TEM $\leftrightarrow$ ITG dominance transition in the matched profile case.

Finally, application of the linear mode quasilinear transport approximation implicates that a change in the mix of mode saturation levels given by a TEM population collapse underlies the observed bistability of turbulent fluctuations and momentum transport. For a full understanding of the turbulent populations at the LOC/SOC transition, future work should address the validity of these quasilinear approximations, and address the mechanism of bistability.

## Acknowledgments

We acknowledge Nathan T. Howard and Francesco Sciortino for their helpful advice on this work, and also fruitful discussions at the 2018 Chengdu Theory Festival. This work was supported by the U.S. Department of Energy, Office of Science, Office of Fusion Energy Sciences under Award Numbers DE-FG02-04ER54738, DE-SC0014264, DE-FC02-99ER54512.

- [1] Duval B P, Bortolon A, Karpushov A, Pitts R A, Pochelon A, Sauter O, Scarabosio A and Turri G 2008 *Physics of Plasmas* **15** 056113 ISSN 1070-664X
- [2] Rice J E, Cziegler I, Diamond P H, Duval B P, Podpaly Y A, Reinke M L, Ennever P C, Greenwald M J, Hughes J W, Ma Y, Marmor E S, Porkolab M, Tsujii N and Wolfe S M 2011 *Physical Review Letters* **107** 265001 ISSN 0031-9007
- [3] Angioni C, McDermott R M, Casson F J, Fable E, Bottino A, Dux R, Fischer R, Podoba Y, Pütterich T, Ryter F and Viezzer E 2011 *Physical Review Letters* **107** 215003 ISSN 0031-9007
- [4] Grierson B A, Chrystal C, Haskey S R, Wang W X, Rhodes T L, McKee G R, Barada K, Yuan X, Nave M F F, Ashourvan A and Holland C 2019 *Physics of Plasmas* **26** 042304 ISSN 1070-664X
- [5] Diamond P H, Liang Y M, Carreras B A and Terry P W 1994 *Physical Review Letters* **72** 2565–2568 ISSN 0031-9007
- [6] Romanelli F, Tang W and White R 1986 *Nuclear Fusion* **26** 1515–1528 ISSN 0029-5515
- [7] Erofeev I, Fable E, Angioni C and McDermott R 2017 *Nuclear Fusion* **57** 126067 ISSN 0029-5515
- [8] Arnichand H, Sabot R, Hacquin S, Krämer-Flecken A, Garbet X, Citrin J, Bourdelle C, Hornung G, Bernardo J, Bottereau C, Clairet F, Falchetto G and Giacalone J 2014 *Nuclear Fusion* **54** 123017 ISSN 0029-5515
- [9] Shi Y, Kwon J, Diamond P, Ko W, Choi M, Ko S, Hahn S, Na D, Leem J, Lee J, Yang S, Lee K, Joung M, Jeong J, Yoo J, Lee W, Lee J, Bae Y, Lee S, Yoon S, Ida K and Na Y S 2017 *Nuclear Fusion* **57** 066040 ISSN 0029-5515
- [10] Angioni C, Peeters A G, Ryter F, Jenko F, Conway G D, Dannert T, Fahrbach H U, Reich M, Suttrop W, ASDEX Upgrade Team and Fattorini L 2005 *Physics of Plasmas* **12** 040701 ISSN 1070-664X
- [11] Camenen Y, Angioni C, Bortolon A, Duval B P, Fable E, Hornsby W A, McDermott R M, Na D H, Na Y S, Peeters A G and Rice J E 2017 *Plasma Physics and Controlled Fusion* **59** 034001 ISSN 0741-3335 (*Preprint* 1701.08095)
- [12] Peeters A G and Angioni C 2005 *Physics of Plasmas* **12** 072515 ISSN 1070-664X
- [13] Diamond P H, McDevitt C J, Gürçan Ö D, Hahn T S and Naulin V 2008 *Physics of Plasmas* **15** 012303 ISSN 1070-664X
- [14] Peeters A, Angioni C, Bortolon A, Camenen Y, Casson F, Duval B, Fiederspiel L, Hornsby W, Idomura Y, Hein T, Kluy N, Mantica P, Parra F, Snodin A, Szepesi G, Strintzi D, Tala T, Tardini G, de Vries P and Weiland J 2011 *Nuclear Fusion* **51** 094027 ISSN 0029-5515
- [15] Wang L and Diamond P H 2013 *Physical Review Letters* **110** 265006 ISSN 0031-9007
- [16] Kosuga Y, Diamond P H and Gürçan Ö D 2010 *Physics of Plasmas* **17** 102313 ISSN 1070-664X
- [17] Diamond P, Kosuga Y, Gürçan Ö, McDevitt C, Hahn T, Fedorczak N, Rice J, Wang W, Ku S,

- Kwon J, Dif-Pradalier G, Abiteboul J, Wang L, Ko W, Shi Y, Ida K, Solomon W, Jhang H, Kim S, Yi S, Ko S, Sarazin Y, Singh R and Chang C 2013 *Nuclear Fusion* **53** 104019 ISSN 0029-5515
- [18] Wang W X, Diamond P H, Hahm T S, Ethier S, Rewoldt G and Tang W M 2010 *Physics of Plasmas* **17** 072511 ISSN 1070-664X
- [19] Kwon J, Yi S, Rhee T, Diamond P, Miki K, Hahm T, Kim J, Gürçan Ö and McDevitt C 2012 *Nuclear Fusion* **52** 013004 ISSN 0029-5515
- [20] Grierson B A, Wang W X, Ethier S, Staebler G M, Battaglia D J, Boedo J A, DeGrassie J S and Solomon W M 2017 *Physical Review Letters* **118** 015002 ISSN 0031-9007
- [21] Sung C, White A, Howard N, Oi C, Rice J, Gao C, Ennever P, Porkolab M, Parra F, Mikkelsen D, Ernst D, Walk J, Hughes J, Irby J, Kasten C, Hubbard A and Greenwald M 2013 *Nuclear Fusion* **53** 083010 ISSN 0029-5515
- [22] Sung C, White A E, Mikkelsen D R, Greenwald M, Holland C, Howard N T, Churchill R and Theiler C 2016 *Physics of Plasmas* **23** 042303 ISSN 1070-664X
- [23] McDermott R, Angioni C, Conway G, Dux R, Fable E, Fischer R, Pütterich T, Ryter F and Viezzer E 2014 *Nuclear Fusion* **54** 043009 ISSN 0029-5515
- [24] Bortolon A, Duval B P, Pochelon A and Scarabosio A 2006 *Physical Review Letters* **97** 235003 ISSN 0031-9007
- [25] Rice J, Duval B, Reinke M, Podpaly Y, Bortolon A, Churchill R, Cziegler I, Diamond P, Dominguez A, Ennever P, Fiore C, Granetz R, Greenwald M, Hubbard A, Hughes J, Irby J, Ma Y, Marmor E, McDermott R, Porkolab M, Tsujii N and Wolfe S 2011 *Nuclear Fusion* **51** 083005 ISSN 0029-5515
- [26] Greenwald M, Bader A, Baek S, Bakhtiari M, Barnard H, Beck W, Bergerson W, Bespamyatnov I, Bonoli P, Brower D, Brunner D, Burke W, Candy J, Churchill M, Cziegler I, Diallo A, Dominguez A, Duval B, Edlund E, Ennever P, Ernst D, Faust I, Fiore C, Fredian T, Garcia O, Gao C, Goetz J, Golfinopoulos T, Granetz R, Grulke O, Hartwig Z, Horne S, Howard N, Hubbard A, Hughes J, Hutchinson I, Irby J, Izzo V, Kessel C, LaBombard B, Lau C, Li C, Lin Y, Lipschultz B, Loarte A, Marmor E, Mazurenko A, McCracken G, McDermott R, Meneghini O, Mikkelsen D, Mossessian D, Mungaard R, Myra J, Nelson-Melby E, Ochoukov R, Olynk G, Parker R, Pitcher S, Podpaly Y, Porkolab M, Reinke M, Rice J, Rowan W, Schmidt A, Scott S, Shiraiwa S, Sierchio J, Smick N, Snipes J A, Snyder P, Sorbom B, Stillerman J, Sung C, Takase Y, Tang V, Terry J, Terry D, Theiler C, Tronchin-James A, Tsujii N, Vieira R, Walk J, Wallace G, White A, Whyte D, Wilson J, Wolfe S, Wright G, Wright J, Wukitch S and Zweben S 2014 *Physics of Plasmas* **21** 110501 ISSN 1070-664X
- [27] Chilenski M, Greenwald M, Marzouk Y, Howard N, White A, Rice J and Walk J 2015 *Nuclear Fusion* **55** 023012 ISSN 0029-5515
- [28] Rice J, Gao C, Reinke M, Diamond P, Howard N, Sun H, Cziegler I, Hubbard A, Podpaly Y, Rowan W, Terry J, Chilenski M, Delgado-Aparicio L, Ennever P, Ernst D, Greenwald M, Hughes J, Ma Y, Marmor E, Porkolab M, White A and Wolfe S 2013 *Nuclear Fusion* **53** 033004 ISSN 0029-5515
- [29] Candy J, Belli E and Bravenec R 2016 *Journal of Computational Physics* **324** 73–93 ISSN 00219991
- [30] Kwak D D J 2015 *Investigation of intrinsic rotation dependencies in Alcator C-Mod using a new data analysis workflow* Master's thesis Massachusetts Institute of Technology
- [31] Waltz R E, Casati A and Staebler G M 2009 *Physics of Plasmas* **16** 072303 ISSN 1070-664X
- [32] White A E, Peebles W A, Rhodes T L, Holland C H, Wang G, Schmitz L, Carter T A, Hillesheim J C, Doyle E J, Zeng L, McKee G R, Staebler G M, Waltz R E, DeBoo J C, Petty C C and Burrell K H 2010 *Physics of Plasmas* **17** 056103 ISSN 1070-664X
- [33] Freethy S J, Görler T, Creely A J, Conway G D, Denk S S, Happel T, Koenen C, Hennequin P and White A E 2018 *Physics of Plasmas* **25** 055903 ISSN 1070-664X
- [34] Staebler G M, Kinsey J E and Waltz R E 2007 *Physics of Plasmas* **14** 055909 ISSN 1070-664X
- [35] Bourdelle C, Garbet X, Imbeaux F, Casati A, Dubuit N, Guirlet R and Parisot T 2007 *Physics of Plasmas* **14** 112501 ISSN 1070-664X

- [36] Hawryluk R 1981 An Empirical Approach to Tokamak Transport *Physics of Plasmas Close to Thermonuclear Conditions* (Elsevier) pp 19–46 ISBN 9781483283852
- [37] Belli E A and Candy J 2008 *Plasma Physics and Controlled Fusion* **50** 095010 ISSN 0741-3335
- [38] Rodriguez-Fernandez P, White A E, Howard N T, Grierson B A, Staebler G M, Rice J E, Yuan X, Cao N M, Creely A J, Greenwald M J, Hubbard A E, Hughes J W, Irby J H and Sciortino F 2018 *Physical Review Letters* **120** 075001 ISSN 0031-9007
- [39] Hornung G, Dif-Pradalier G, Clairet F, Sarazin Y, Sabot R, Hennequin P and Verdoolaege G 2017 *Nuclear Fusion* **57** 014006 ISSN 0029-5515